

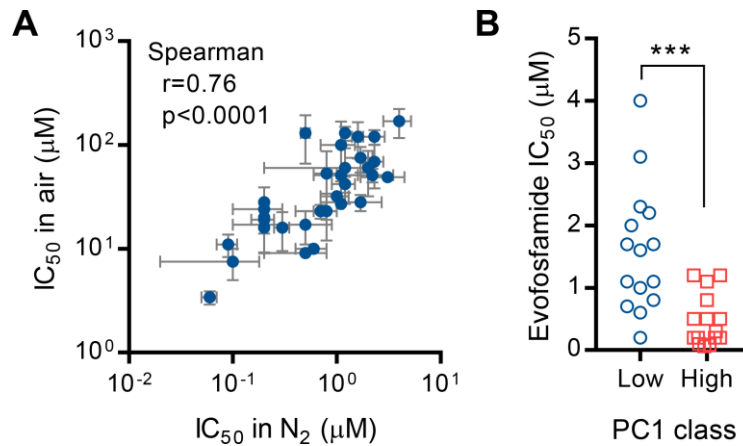
Molecular Pharmacology

Supplemental Figures for

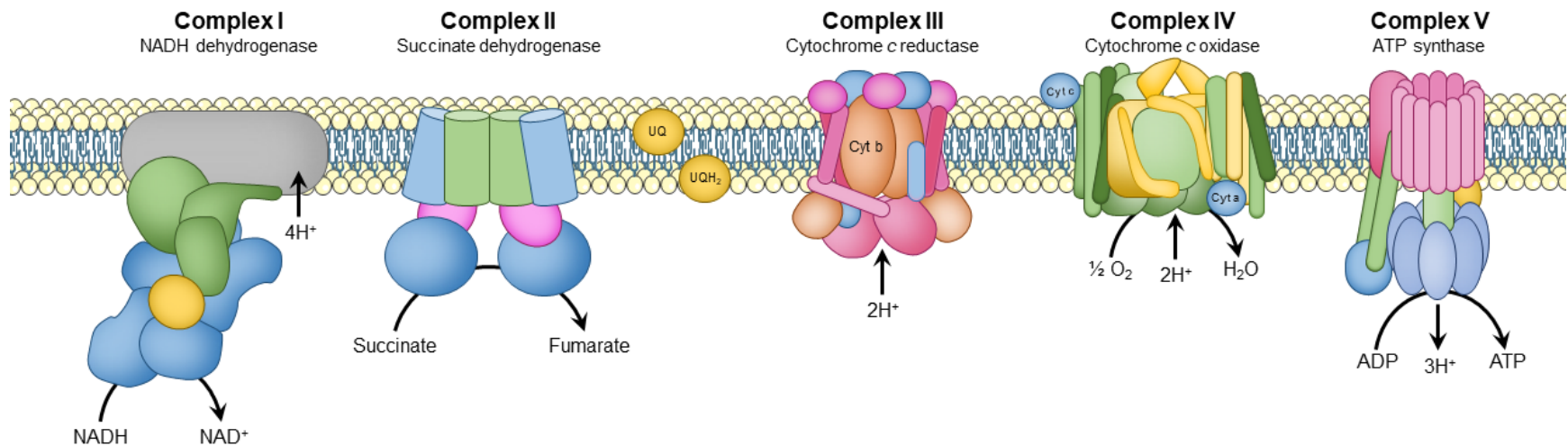
Functional CRISPR and shRNA screens identify involvement of mitochondrial electron transport in the activation of evofosfamide

Francis W. Hunter, Jules B. L. Deveaux, Fanying Meng, Cho Rong Hong, Peter Tsai, Troy W. Ketela, Indumati Sharma, Purvi R. Kakadia, Aziza Khan, Stefano Marastoni, Zvi Shalev, Anthony J. R. Hickey, Charles P. Hart, Cristin G. Print, Stefan K. Bohlander, Bradly G. Wouters, William R. Wilson

*Corresponding author email: f.hunter@auckland.ac.nz



Supplemental Figure 1. (A) Correlation between the sensitivity of 32 cancer cell lines to evofosfamide when challenged under anoxia (“N₂”) or 20% O₂ (“air”) and as assessed by 7-d regrowth assay. Data points are the mean + SEM of IC₅₀ determinations from three independent experiment for each cell line. Data correspond to Figure 1B in the main text. (B) Comparison of evofosfamide sensitivity under anoxia between cell lines dichotomised by the first principal component of expression values for 173 genes correlated with evofosfamide potency (Pearson coefficient <math><-0.4</math>; illustrated in Figure 2B in the main text). Statistical significance of differences in the distribution of IC₅₀ values between groups was assessed by Mann–Whitney U-test.



NADH dehydrogenase

E	ND1	ND2	ND3	ND4	ND4L	ND5	ND6										
E	Ndufs1	Ndufs2	Ndufs3	Ndufs4	Ndufs5	Ndufs6	Ndufs7	Ndufs8	Ndufv1	Ndufv2	Ndufv3						
B/A	NuoA	NuoB	NuoC	NuoD	NuoE	NuoF	NuoG	NuoH	NuoI	NuoJ	NuoK	NuoL	NuoM	NuoN			
B/A	NdhC	NdhK	NdhJ	NdhH	NdhA	NdhI	NdhG	NdhE	NdhF	NdhD	NdhB	NdhL	NdhM	NdhN	HoxE	HoxF	HoxJ
E	Ndufa1	Ndufa2	Ndufa3	Ndufa4	Ndufa5	Ndufa6	Ndufa7	Ndufa8	Ndufa9	Ndufa10	Ndufab1	Ndufa11	Ndufa12	Ndufa13			
E	Ndubf1	Ndubf2	Ndubf3	Ndubf4	Ndubf5	Ndubf6	Ndubf7	Ndubf8	Ndubf9	Ndubf10	Ndubf11	Ndufc1	Ndufc2				

Succinate dehydrogenase / Fumarate reductase

E	SDHC	SDHD	SDHA	SDHB
B/A	SdhC	SdhD	SdhA	SdhB
	FrdA	FrdB	FrdC	FrdD

Cytochrome c reductase

E/B/A	ISP	Cyt b	Cyt 1				
E	COR1	QCR2	QCR6	QCR7	QCR8	QCR9	QCR10

Cytochrome c oxidase

E	COX10	COX3	COX1	COX2	COX4	COX5A	COX5B	COX6A	COX6B	COX6C	COX7A	COX7B	COX7C	COX8	E/B/A	COX11	COX15	COX17
B/A	CyoE	CyoD	CyoC	CyoB	CyoA													
	CoxD	CoxC	CoxA	CoxB														
	QoxD	QoxC	QoxB	QoxA														

Cytochrome c oxidase, cbb3-type

B	I	II	IV	III
---	---	----	----	-----

Cytochrome bd complex

B/A	CydA	CydB	CydX
-----	------	------	------

F-type ATPase (Bacteria)

alpha	beta	gamma	delta	epsilon
a	b	c		

F-type ATPase (Eukaryotes)

alpha	beta	gamma	delta	epsilon	
OSCP	a	b	c	d	e
f	g	fb/h	j	k	8

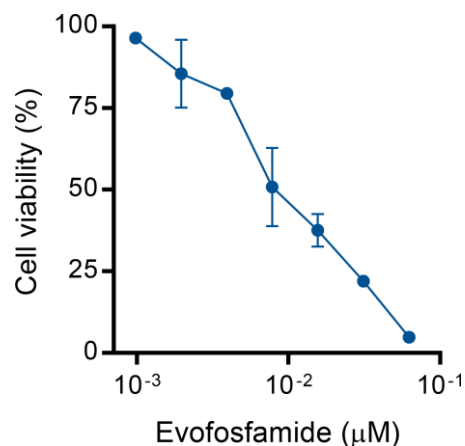
V/A-type ATPase (Bacteria, Archaeas)

A	B	C	D	E	F	G/H
I	K					

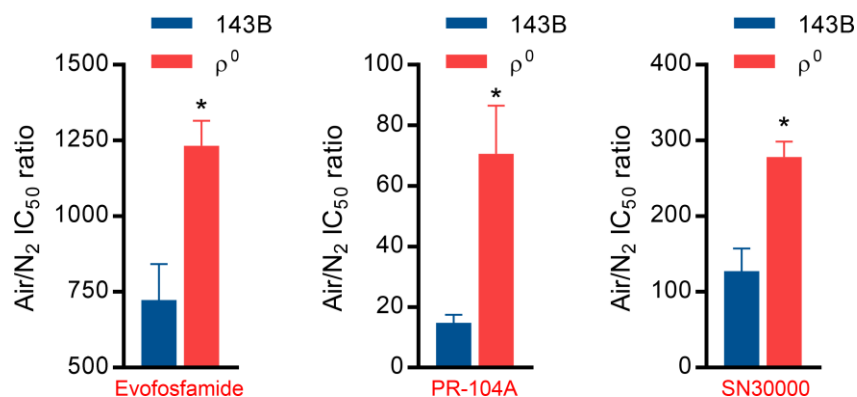
V-type ATPase (Eukaryotes)

A	B	C	D	E	F	G	H
a	c	d	e	S1			

Supplemental Figure 2. Mitochondrial electron transport chain components correlated with evofosfamide potency in 30 genomically diverse cancer cell lines. The expression of all genes marked with red stars correlated with evofosfamide potency (Pearson coefficient <-0.4).



Supplemental Figure 3. Concentration-dependent inhibition of cell viability in KBM-7 cells exposed to evofosfamide. Cells (2,000 per well in 96-well format) were challenged with an evofosfamide dilution series under anoxia for 2 h, re-oxygenated then cultured for 5 d before assessing viability using alamarBlue. Data points are the mean \pm SEM of determinations from three independent experiments.



Supplemental Figure 4. Hypoxia selectivity of evofosfamide, PR-104A and SN30000 in parental and ρ^0 143B osteosarcoma cells. Data are the mean + SEM of the intra-experiment ratio of IC₅₀ values for cells challenged with evofosfamide under 20% O₂ (“air”) or anoxia (“N₂”) in three independent pairs of assays. Statistical significance of differences in IC₅₀ ratios was assessed by Mann–Whitney U-test.